Michael W. Miller*, Elizabeth S. Williams†
**Colorado Division of Wildlife, Wildlife Research Center, Fort Collins, Colorado 80526, USA*
e-mail: mike.miller@state.co.us
†Department of Veterinary Sciences, University of Wyoming, Laramie, Wyoming 82070, USA

1. Prusiner, S. B. *Proc. Natl Acad. Sci. USA* **95,** 13363–13383 (1998).
2. McFadyean, J. *J. Comp. Pathol. Ther.* **31,** 102–131 (1918).
3. Hourrigan, J., Klingsporn, A., Clark, W. W. & de Camp, M. in *Slow Transmissible Diseases of the Nervous System:* Vol. 1 (eds Prusiner, S. B. & Hadlow, W. J.) 331–356 (Academic, New York, 1979).
4. Williams, E. S. & Young, S. *Rev. Sci. Tech. Off. Int. Epiz.* **11,** 551–567 (1992).
5. Hoinville, L. J. *Rev. Sci. Tech. Off. Int. Epiz.* **15,** 827–852 (1996).
6. Woolhouse, M. E. J., Stringer, S. M., Matthews, L., Hunter, N. & Anderson, R. M. *Proc. R. Soc. Lond. B* **265,** 1205–1210 (1998).
7. Miller, M. W. *et al. J. Wildl. Dis.* **36,** 676–690 (2000).
8. Williams, E. S. & Miller, M. W. *Rev. Sci. Tech. Off. Int. Epiz.* **21,** 305–316 (2002).
9. Redman, C. A. *et al. Epidemiol. Infect.* **128,** 513–521 (2002).
10. Sigurdson, C. J. *et al. J. Gen. Virol.* **80,** 2757–2764 (1999).
11. Spraker, T. R. *et al. Vet. Pathol.* **39,** 110–119 (2002).
12. Hadlow, W. J., Kennedy, R. C. & Race, R. E. *J. Infect. Dis.* **146,** 657–664 (1982).

Competing financial interests: declared none.

Nanotube electronics

Large-scale assembly of carbon nanotubes

Nanoscale electronic devices made from carbon nanotubes, such as transistors and sensors[1–5], are much smaller and more versatile than those that rely on conventional microelectronic chips, but their development for mass production has been thwarted by difficulties in aligning and integrating the millions of nanotubes required. Inspired by biomolecular self-assembly processes, we have created chemically functionalized patterns on a surface, to which pre-grown nanotubes in solution can align themselves in huge numbers. This method allows wafer-scale fabrication of millions of carbon-nanotube circuits with single-nanotube precision, and may enable nanotube-based devices, such as computer chips and high-density sensor arrays, to be produced industrially.

We used organic molecular marks on a substrate to guide the self-assembly of individual single-walled carbon nanotubes (swCNTs; see supplementary information). In the surface-functionalization step, we created two distinct surface regions coated either with polar chemical groups (such as amino ($–NH_2$/$–NH_3^+$) or carboxyl ($–COOH$/$–COO^-$)) or with non-polar groups (such as methyl ($–CH_3$)). We achieved this by direct deposition of proper organic molecules (for example, as a self-assembled monolayer) by dip-pen nanolithography[6–8] or by microcontact stamping[9]. These deposition techniques enabled us to functionalize the substrates without resorting to intermediate chemical steps, thereby minimizing surface contamination.

When the substrate is placed in a suspension of swCNTs, the nanotubes are attracted towards the polar regions and self-assemble to form predesigned structures, usually within about 10 s. We used a magnet to remove common magnetic nanoparticle impurities from swCNT suspensions to improve the reliability of the process.

We discovered that a lateral-directional force exists on swCNTs near the boundary between the polar and non-polar molecular regions (Fig. 1a). This force, which presumably originates from electrostatic interactions, rotates the swCNTs towards the polar region and confines them to the inside of it (Fig. 1a, inset).

Previous methods have relied on external forces, such as electric or magnetic fields, and liquid flow to align nanowires precisely[10–13]. However, it is time-consuming to align millions of randomly oriented nanotube circuits by using external forces. In our process, individual polar molecular marks attract and align swCNTs along pre-determined lines without external force, enabling any swCNT-based structure to be assembled simply by using polar molecular patterns with the required shapes.

We scaled up this process for high-throughput assembly. In principle, large numbers of microscale molecular patterns can easily be generated over a large chip area by using high-throughput patterning methods such as photolithography, stamping and, in the future, parallel dip-pen nanolithography[8].

Our assembly of millions of individual swCNTs on stamp-generated microscale patterns that cover areas of about 1 cm^2 on gold, for example, occurs with a yield of more than 90% (Fig. 1b). Surprisingly, we found that in swCNT suspensions at low concentrations (for example, about 0.02 mg ml^{-1} in 1,2-dichlorobenzene), only a single nanotube lies at the centre of each microscale polar molecular pattern, even though there is enough room for more nanotubes to assemble (Fig. 1b, inset). We used height profiles, determined by atomic-force microscopy, to confirm that assembly originated from one nanotube. Presumably, the hydrophobic surface of the swCNT passivates the polar pattern on the substrate and reduces the likelihood of adhesion by additional swCNTs.

We incorporated this process into conventional microfabrication methods to make millions of swCNT-based circuits over areas of about 1 cm^2. Individual swCNTs are assembled between two polar molecular patterns generated by stamping on microfabricated gold electrodes. We used short (about 1 nm) polar molecules with π-electrons (such as 2-mercaptoimidazole) to minimize the contact resistance between the nanotubes and the electrodes. Atomic-force microscopy, using a conducting probe, confirmed the existence of stable swCNT circuits that conducted micro-ampere currents.

Figure 1c shows that more than 70% of the junctions are connected by only one swCNT. This proportion should increase as swCNT-purification processes advance or as the gap size is reduced for high-density integration (for example, a roughly 90% yield on flat surfaces). High-precision assembly should then enable swCNTs to be used in practical applications.

Saleem G. Rao, Ling Huang, Wahyu Setyawan, Seunghun Hong*
Department of Physics, Center for Materials Research and Technology and Institute of Molecular Biophysics, Florida State University, Tallahassee, Florida 32306, USA
**Present address: Department of Physics, Seoul National University, Seoul 151-742, South Korea*
e-mail: shong@phya.snu.ac.kr

1. Tans, S. J. *et al. Nature* **386,** 474–477 (1997).
2. Lee, J. *et al. Nature* **415,** 1005–1008 (2002).
3. Kong, J., Soh, H. T., Cassell, A. M., Quate, C. F. & Dai, H. *Nature*

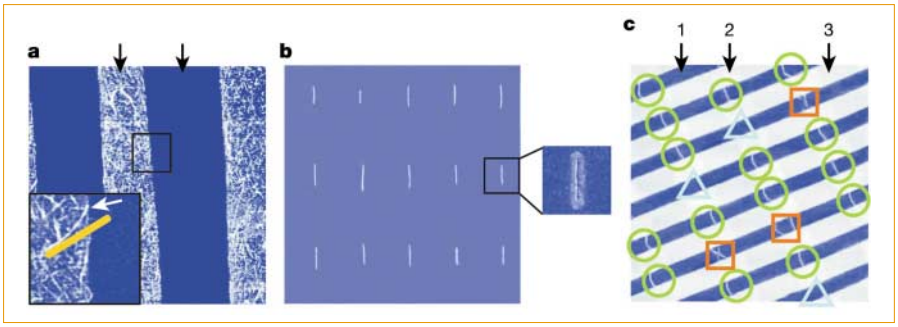

Figure 1 Atomic-force micrographs showing large-scale self-assembly of single-walled carbon nanotubes (swCNTs). **a,** Image (12 × 12 μm^2) showing the topography of swCNTs near the boundary (white arrow, inset) between polar (cysteamine; left arrow) and non-polar (1-octadecanethiol (ODT); right arrow) molecular patterns on gold. No swCNTs are evident in ODT regions. Yellow bar represents a tangent to a bent swCNT, showing the extent of bending due to lateral–directional force. **b,** Topography (30 × 30 μm^2) of an array of individual swCNTs covering about 1 cm^2 of gold surface. The friction-force image (inset) shows a single swCNT (dark line), and the regions containing 2-mercaptoimidazole (bright area) and ODT (dark area). **c,** Topography (20 × 20 μm^2) of an array of junctions with no swCNTs (triangles), one swCNT (circles) or two swCNTs (squares), covering an area of about 1 cm^2. Arrows 1, 2 and 3 indicate octadecyltrichlorosilane (used to passivate the SiO_2 surface), 2-mercaptoimidazole on gold, and ODT on gold, respectively.

395, 878–881 (1998).
4. Fuhrer, M. S. *et al. Science* **288,** 494–497 (2000).
5. Bockrath, M. *et al. Science* **291,** 283–285 (2001).
6. Hong, S. & Mirkin, C. A. *Science* **288,** 1808–1811 (2000).
7. Manandhar, P. *et al. Phys. Rev. Lett.* **90,** 115505 (2003).
8. Zhang, M. *et al. Nanotechnology* **13,** 212–217 (2002).
9. Xia, Y. & Whitesides, G. M. *J. Am. Chem. Soc.* **117,** 3274–3275 (1995).
10. Liu, J. *et al. Chem. Phys. Lett.* **303,** 125–129 (1999).
11. Chen, X. Q., Saito, T., Yamada, H. & Matsushige, K. *Appl. Phys. Lett.* **78,** 3714–3716 (2001).
12. Hone, J. *et al. Appl. Phys. Lett.* **77,** 666–668 (2000).
13. Huang, Y., Duan, X. F., Wei, Q. Q. & Lieber, C. M. *Science* **291,** 630–633 (2001).

Supplementary information accompanies this communication on *Nature*'s website.
Competing financial interests: declared none.

Innate defence

Evidence for memory in invertebrate immunity

Acquired immunity in vertebrates is characterized by immunological memory and specificity, whereas the innate defence systems of invertebrates are assumed to have no specific memory[1–3]. Here we use a model system of a copepod, which is a minute crustacean, and a parasitic tapeworm to show that the success of reinfection depends on the antigenic resemblance between the consecutively encountered parasites. This finding indicates that an invertebrate defence system may be capable of specific memory.

The degree of specificity and memory in invertebrate immunity is unclear[3–5]. Although a defence reaction can be induced in invertebrates against pathogens[6], the responses may not be specific as they are able to distinguish only between different classes of pathogen[2,3]. However, genotype-specific interactions between invertebrate hosts and different lines of parasites are possible[4,7]. Such coevolutionary phenomena are difficult to explain unless there is some specificity in the immune system.

We investigated the line-specific memory of the defence system of an invertebrate host, the copepod *Macrocyclops albidus*, against a natural parasite, the tapeworm *Schistocephalus solidus*. To vary the antigenic features of the pathogen presented to the host, we exposed each copepod to three tapeworm larvae and then either to three sibling parasites or to unrelated parasites of a different sib-group three days later (Fig. 1a). All tapeworms used for the second exposure were fluorescently labelled to distinguish them from the parasites used for primary infection[8].

If there is a specific memory inherent in the defence by the copepod hosts, we would expect a reduction in the success of reinfection by the sibling parasites. Indeed, we found that prior exposure to related parasites resulted in less secondary infection than occurred after exposure to unrelated parasites (Fig. 1b). On average, the reinfection success was reduced from $59.5 \pm 3.5\%$ to $47.6 \pm 4.8\%$ of copepods infected (paired t-test, $t = 3.236$, $n = 24$, $P = 0.0037$). In addition, the average intensity of reinfection decreased from 0.81 ± 0.06 to 0.66 ± 0.07 tapeworms per host ($t = 2.723$, $n = 24$, $P = 0.0121$). This effect should increase with the antigenic similarity between the consecutively encountered parasites.

Because the tapeworms are simultaneous hermaphrodites whose self-fertilization (selfing) leads to homogeneous offspring, we compared the size of the host's 'memory' effect towards tapeworms produced by selfing against that for tapeworms produced by outcrossing. As predicted, the reduction in reinfection increased for selfed worms (Fig. 1c; t-test, $n = 8$; $n = 16$ for outcrossed worms; reinfection success, $t = 1.361$, $P = 0.187$; intensity, $t = 2.230$, $P = 0.036$).

Could this reduced reinfection be due to factors other than the host defence system? Neither host mortality nor primary infection (determined in 16 of the 24 sibships) differed between treatments (nominal logistic models, $P > 0.2$). Could the parasites themselves cause the reduction in reinfection? This is unlikely because cooperation between kin should facilitate rather than reduce reinfection.

If within-host competition between siblings is particularly strong, only those hosts that did not clear the primary infection would be affected. Excluding hosts with a resident primary infection from our sample did not diminish the effect: prior exposure to sib-group parasites still reduced reinfection from 64.1% to 45.6% in this smaller sample (in a nominal logistic model, including sibship, the effect of previous exposure was $\chi^2_1 = 7.728$, $n = 128$, $P = 0.0054$). We conclude that parasite-derived effects are unlikely to explain the observed reduction in reinfection after consecutive exposure of the host to related parasites.

Our results show that the defence system of copepods can react more efficiently after it has previously encountered antigenically similar parasites. To our knowledge, this

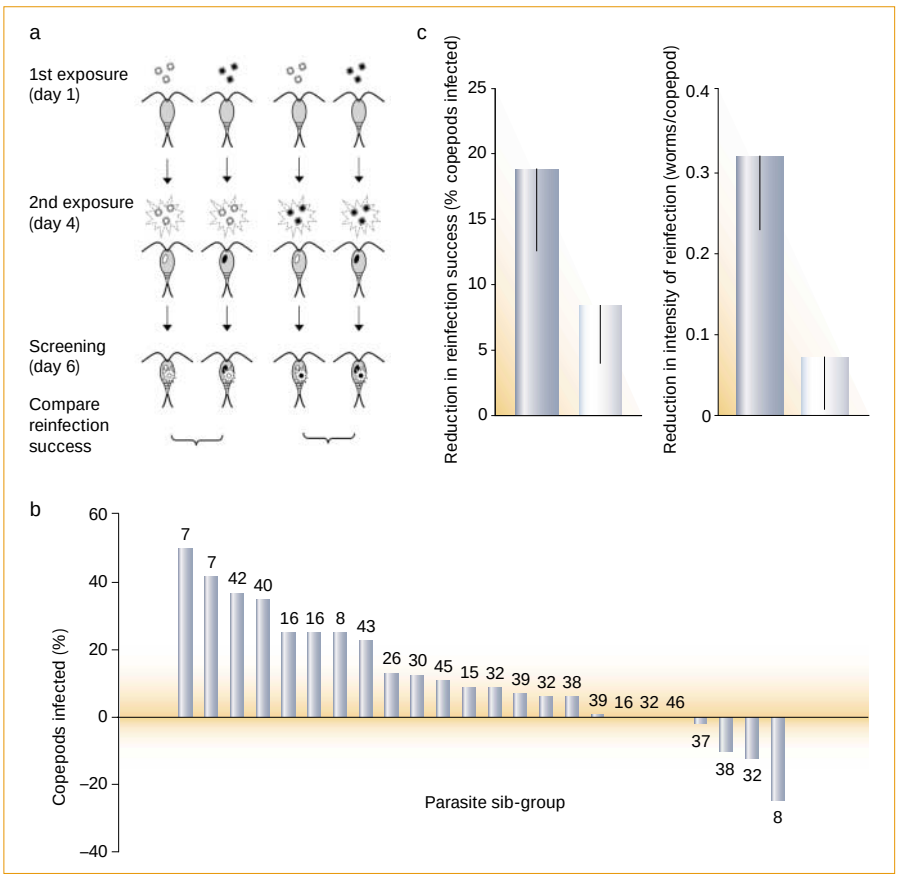

Figure 1 Exposure of a copepod to a tapeworm parasite reduces the chances of reinfection by antigenically similar tapeworm larvae. **a,** Experimental design. Two parasite sib-groups are shown (denoted by white and black larvae). There were $n = 24$ sib-groups, which varied in infectivity (nominal logistic model, $\chi^2_{23} = 95.95$, $n = 684$, $r^2 = 0.102$, $P < 0.001$). The experiment was reproduced in two rounds, both of which gave similar results and so were combined. Comparisons are made within the same parasite sib-group to control for variation in infectivity (further details are available from the authors). **b,** Reduction in reinfection due to prior exposure of the copepod host to sibling parasites, compared with exposure to unrelated tapeworms, for each of the 24 tapeworm sib-groups (arranged in rank order of difference). Sample sizes (number of copepods) are indicated above each bar. **c,** Difference in the success (left) and intensity (right) of copepod reinfection due to the degree of antigenic resemblance between tapeworm larvae used for reinfection and those used for primary infection. Left bars, selfed larvae; right bars, outcrossed larvae. Standard errors are indicated.